Monolithic Two-Terminal III–V//Si Triple-Junction Solar Cells With 30.2% Efficiency Under 1-Sun AM1.5g

Romain Cariou, Jan Benick, Paul Beutel, Nasser Razek, Christoph Flötgen, Martin Hermle, David Lackner, Stefan W. Glunz, *Senior Member, IEEE*, Andreas W. Bett, *Member, IEEE*, Markus Wimplinger, and Frank Dimroth, *Member, IEEE*

***Abstract*—Stacking III–V p-n junctions on top of wafer-based silicon solar cells is a promising way to go beyond the silicon single-junction efficiency limit. In this study, triple-junction GaInP/$Al_x Ga_{1-x}$As//Si solar cells were fabricated using surface-activated direct wafer bonding. Metal–organic-vapor-phase-epitaxy-grown GaInP/$Al_x Ga_{1-x}$As top cells are bonded at low temperature to independently prepared wafer-based silicon cells. n-Si//n-GaAs interfaces were investigated and achieved bulk-like bond strength, high transparency, and conductivity homogeneously over 4-inch wafer area. We used transfer-matrix optical modeling to identify the best design options to reach current-matched two-terminal devices with different mid-cell bandgaps (1.42, 1.47, and 1.52 eV). Solar cells were fabricated accordingly and calibrated under AM1.5g 1-sun conditions. An improved Si back-side passivation process is presented, leading to a current density of 12.4 mA/cm^2 (AM1.5g), measured for a flat Si cell below GaAs. The best 4 cm^2 GaInP/GaAs//Si triple-junction cell reaches 30.2% 1-sun efficiency.**

***Index Terms*—Photovoltaic cells, silicon, III-V semiconductor materials.**

I. Introduction

IMPROVING power conversion efficiency has been driving research for years, since it has a major impact on electricity generation cost. Monocrystalline silicon, the dominant technology on the photovoltaic (PV) market, benefits from a well-established industry. However, with the present record power conversion efficiency of 26.3% [1], there is very little room for Si cell improvement. On the other hand, much higher efficiencies have been achieved through the reduction of transmission and thermalization losses by stacking III–V p-n diodes: record efficiency values of 38.8% for 1-sun/five-junctions and 46.0% for 508-suns/four-junctions have been reported [2].

Thus, a hybrid device combining the advantages of III–V multijunction solar cells with the benefits of Si, the most widespread PV material, offers great opportunities. Indeed, realistic conversion efficiencies beyond 35% under 1-sun AM1.5g conditions can be expected for a triple junction (3J) made of GaInP/AlGaAs/Si, with few micrometers of III–V material on top of silicon [3], [4]. However, the issues associated with III–V epitaxial growth on silicon are significant [5].

1) The high thermal expansion coefficient mismatch leads to strain and may result in cracks and bowing.
2) The large lattice mismatch between Si and GaAs ($\sim$4%) creates dislocations and, thus, recombination centers.
3) The transition between nonpolar Si and polar III–V crystals induces antiphase domains.

Although the understanding and control of lattice-mismatched heteroepitaxy has improved over the past years [6]–[10], III–V growth on Si remains challenging. Another attractive approach to overcome heteroepitaxy issues consists in joining independently processed Si and III–V solar cells by bonding/gluing techniques. Such solar cells can be combined either in n-terminal configuration ($n > 2$) by using transparent and insulating mediums to optically couple the subcells [11]–[13] or in series connection (two-terminal) [14]–[16].

In this study, we focus on a two-terminal configuration, which corresponds to the silicon module manufacturing standard and thus would be the best option for implementing silicon wafer-based tandem cells into existing PV module technology. For the realization of two-terminal GaInP/$Al_x Ga_{1-x}$As//Si 3J solar cells, we use surface-activated wafer bonding as well as an alternative technique, the EVG580 ComBond, which enable stable monolithic stacks and preserved crystal quality in each junction. In this work, we present process improvements leading to transparent-conductive void-free bonds over the full 4-inch wafer area. We use transfer-matrix optical modeling to define current-matched stacks with the constraint of a flat III–V//Si bond interface. 4 cm^2 bonded GaInP/$Al_x Ga_{1-x}$As//Si devices are fabricated and characterized by external quantum efficiency (EQE) and calibrated 1-sun AM1.5g *I–V* measurements. Finally, an improved silicon back-side passivation process is presented,

Manuscript received June 10, 2016; revised September 5, 2016; accepted November 7, 2016. Date of current version December 20, 2016. This work was supported by the European Union's Horizon 2020 research and innovation program under the Marie Sklodowska-Curie Grant 655272 and by the Austrian Ministry of Technology under the Austrian Space Applications Program.

R. Cariou, J. Benick, P. Beutel, M. Hermle, D. Lackner, A.W. Bett, and F. Dimroth are with the Fraunhofer Institute for Solar Energy Systems, 79110 Freiburg, Germany (e-mail: romain.cariou@ise.fraunhofer.de; jan.benick@ise.fraunhofer.de; Paul.Beutel@ise.fraunhofer.de; martin.hermle@ise.fraunhofer.de; david.lackner@ise.fraunhofer.de; andreas.bett@ise.fraunhofer.de; frank.dimroth@ise.fraunhofer.de).

N. Razek, C. Flötgen, and M. Wimplinger are with EV Group E. Thallner GmbH, 4782 St. Florian am Inn, Austria (e-mail: N.Razek@EVGroup.com; C.Floetgen@EVGroup.com; M.Wimplinger@EVGroup.com).

S. W. Glunz is with the Fraunhofer Institute for Solar Energy Systems, 79110 Freiburg, Germany, and also with the Laboratory for Photovoltaic Energy Conversion, University of Freiburg, 79085 Freiburg, Germany (e-mail: stefan.glunz@ise.fraunhofer.de).

Color versions of one or more of the figures in this paper are available online at http://ieeexplore.ieee.org.

Digital Object Identifier 10.1109/JPHOTOV.2016.2629840

2156-3381 © 2016 IEEE. Translations and content mining are permitted for academic research only. Personal use is also permitted, but republication/redistribution requires IEEE permission. See http://www.ieee.org/publications_standards/publications/rights/index.html for more information.

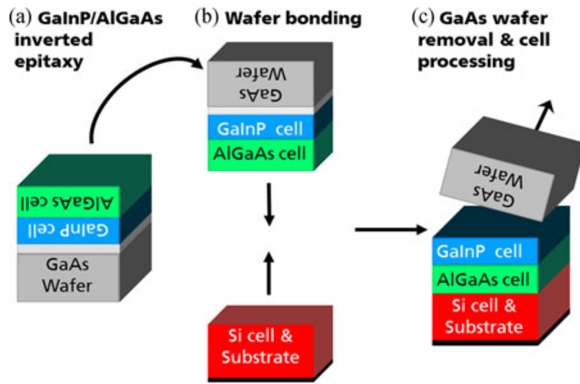

Fig. 1. Process flow for the fabrication of GaInP/AlGaAs//Si 3J wafer-bonded solar cells.

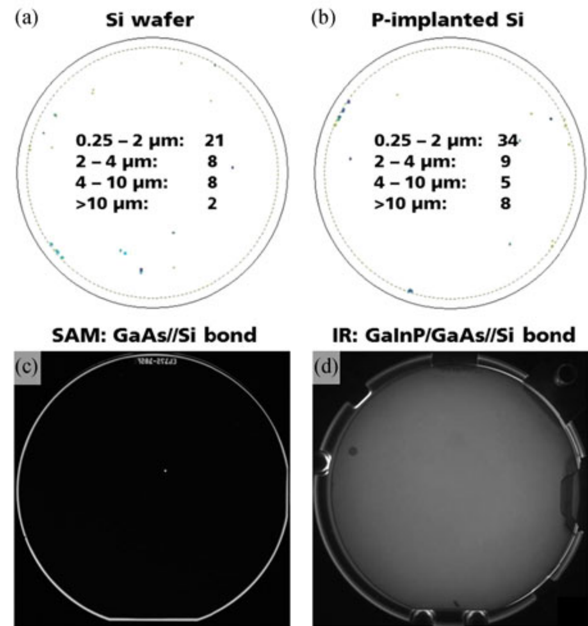

Fig. 2. Particle count (Candela CS20 by KLA Tencor) on 4-inch Si (a) before and (b) after emitter formation. (c) Scanning acoustic microscope image of 4-inch GaAs//Si bonded in Ayumi SAB200. (d) Infrared transmission image of a 3J GaInP/GaAs//Si solar cell bonded in the EVG580 ComBond.

which allows keeping high EQE in the silicon bottom cell and reach high efficiency.

II. Cell Fabrication and Design

An overview of the fabrication process of our wafer-bonded GaInP/Al_xGa_{1-x}As//Si 3J cells is presented in Fig. 1:

1) The $Ga_{0.51}In_{0.49}P/Al_xGa_{1-x}$ As top tandem cells were grown lattice matched with inverted layer direction on 4-inch GaAs substrates using metal–organic vapor phase epitaxy [8]. The silicon bottom cells were prepared independently by implanting phosphorous atoms in p-type float-zone (FZ) c-Si wafers (2 Ω·cm, 280 μm) followed by a high-temperature annealing step in an inert atmosphere.
2) GaAs and Si wafers were then loaded on top and bottom facing electrodes into a 1 × 4” Ayumi SAB200 bond chamber. After reaching a base pressure $<3 \times 10^{-8}$ mbar, the Si and GaAs wafer surfaces were exposed to an argon fast atom beam at a substrate temperature of 120 °C [17]. Effective surface deoxidization was achieved with Ar atoms (kinetic energy 0.3–0.4 keV). The wafers were then brought in contact with a force of 10 kN for a few minutes. For one sample, the novel EVG580 ComBond cluster tool was used with similar process conditions as above. This tool allows for surface oxide removal and reoxidation prevention by operating under high vacuum ambient ($\sim 10^{-8}$ mbar) and provides a significantly higher throughput: up to 20 wafer pairs per hour, thanks to fully automated load-lock and cassette-to-cassette handling.
3) The GaAs growth substrate is then etched away (in $H_2O_2 + NH_4OH$ solution) and the few-micrometers-thick GaInP/Al_xGa_{1-x}As top cells remain on the silicon bottom p-n diode. After this etching step, the silicon rear side was passivated using an Al_2O_3/SiN_x stack, followed by Al evaporation and local rear contacts formation using the laser-fired contact process [18]. Finally, front metal contacts (shading of approximately 3%) are deposited as well as Ta_2O_5/MgF_2 double-layer antireflection coating (resulting in 5% average reflectance for 450–1000-nm wavelength range), and mesa etching (trenches down to $\sim$5 μm inside Si) is performed to isolate individual cells.

To achieve good bond mechanical quality, it is mandatory to bring together nearly perfect surfaces with low roughness ($\lesssim$1 nm) and low particle contamination. Consequently, for the III–V layers, a postdeposition chemical mechanical polishing step was carried out externally at the company III–V Reclaim, prior to bonding. For the silicon bottom cell, the wafer specification easily fulfills the low-roughness requirements, but process steps for emitter formation needed to be carefully reviewed to prevent airborne/solutionborne particle contamination. Indeed, few-micrometers-size particles can induce macroscopic unbonded areas. Thus, the number of process/handling steps for Si prior to bonding was minimized.

As shown in Fig. 2(a), the number of particles found on c-Si by optical surface analysis (Candela CS20 measurement, calibrated on a flat surface with microspheres) is only marginally increased [see Fig. 2(b)] after the process steps for bottom cell emitter formation (phosphorus implantation and annealing). Additionally, a prebonding megasonic cleaning step was performed on both wafer surfaces to further reduce the particle density. With this process flow, nearly void-free bonds over the full 4-inch wafer area are obtained, as visible in Fig. 2(c) with scanning acoustic microscope image of GaAs//Si pairs and in Fig. 2(d) with the GaInP/GaAs//Si infrared transmission image.

Bulk-like bond strength was measured by the Maszara crack opening method for this type of bonds, thus confirming excellent mechanical properties. At the atomic scale, a $\sim$2–3-nm-thin amorphous layer, created by ion bombardment before bonding, is detected in cross-sectional transmission electron microscopic images, as previously published in [19]. Notwithstanding this intermediate layer, very low specific resistance and ohmic characteristics are achieved for n-Si//n-GaAs

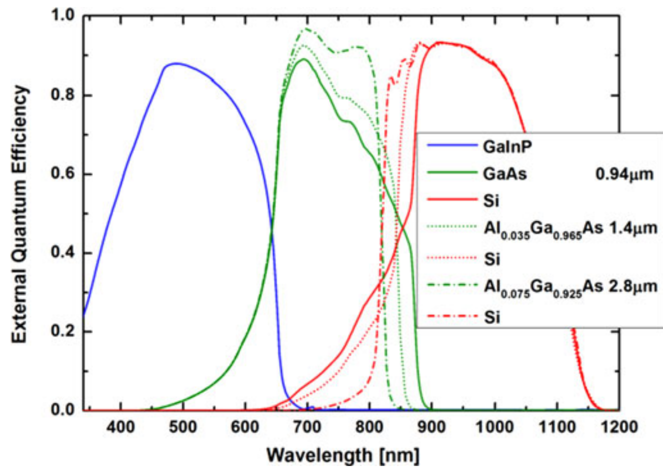

Fig. 3. Transfer-matrix optical modeling of absorption in the GaInP/$Al_xGa_{1-x}As$//Si active solar cell layers with three middle cell Al compositions, including 0%, 3.5%, and 7.5% Al. All three designs are current matched at 12.5 mA/cm^2 under 1-sun AM1.5g.

bonds ($\sim$3 m$\Omega \cdot$ cm^2), thanks to the high doping of the bonding layers: the phosphorous-doped emitter in silicon reaches $N_{\text{surface}} = 5 \times 10^{19}$ cm^{-3} and n-GaAs bond epi-layers has a doping of 1×10^{19} cm^{-3} [17].

In the GaInP/$Al_xGa_{1-x}As$//Si 3J two-terminal configuration, subcell series connection requires current matching of all junctions to get the highest possible efficiency. We have thus used transfer-matrix optical modeling to design 3J cells current matched at a 1-sun current density of 12.5 mA/cm^2 (AM1.5g). This is a realistic target value for a 280-μm planar Si bottom cell below GaAs or AlGaAs.

The optical model includes double-layer magnesium fluoride and tantalum oxide antireflection coating as well as tunnel diodes and a 50-nm GaAs bond layer between the middle and bottom cells (bond layer parasitic absorption $<$0.2 mA/cm^2). Fig. 3 represents the simulated EQE of three devices having the same GaInP top- (500 nm—1.9 eV) and Si bottom cell but with bandgap and thickness variation for the middle $Al_xGa_{1-x}As$ cell: 1) 940 nm of pure GaAs ($E_g = 1.42$ eV); 2) 1400 nm of $Al_{0.035}Ga_{0.965}As$ ($E_g = 1.47$ eV); and 3) 2800 nm of $Al_{0.075}Ga_{0.925}As$ ($E_g = 1.52$ eV). Note that the top cells are designed semitransparent to match the target current density. Those results provide design guidelines to reach 12.5 mA/cm^2 in a GaInP/$Al_xGa_{1-x}As$//Si 3J device. The high-bandgap middle cell offers the highest overall efficiency potential (higher V_{oc}); however, the corresponding thicker absorber requires higher minority carrier diffusion length, which is more challenging; nevertheless, promising results for AlGaAs single-junction solar cells with up to 20% Al were published recently [20].

III. Device Characterization

Based on those modeling results, two types of wafer-bonded 3J devices were first fabricated: one with 3.5% Al in the middle cell ($E_g = 1.47$ eV) and the second with 7.5% Al ($E_g = 1.52$ eV). The final 4 cm^2 devices were measured

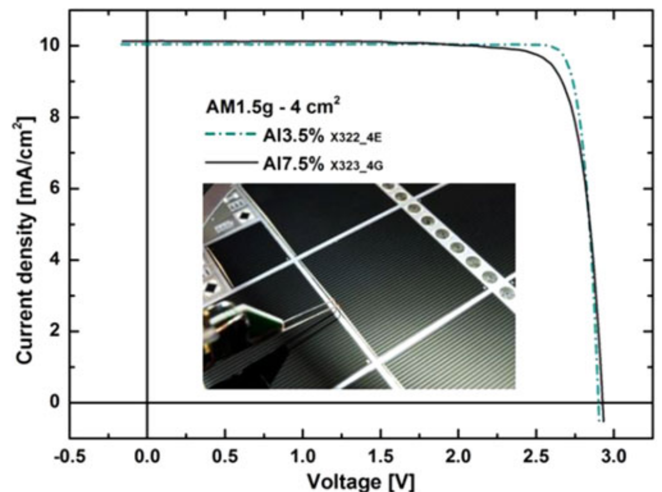

Cell	Aperture Area [cm²]	V_{oc} [mV]	J_{sc} [mA/cm²]	FF [%]	η [%]
Al 3.5% X322_4E	4	2902	10.0	89.8	26.2
Al 7.5% X32_4G	4	2929	10.1	83.1	24.7

(a)

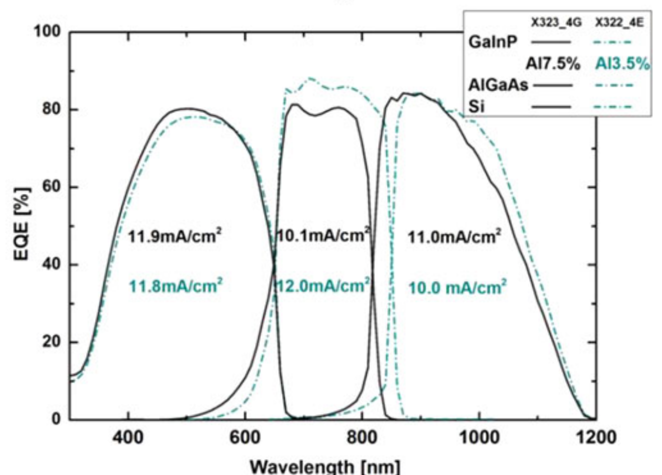

(b)

Fig. 4. (a) AM1.5g *I–V* characteristics of 4 cm^2 wafer-bonded GaInP/$Al_xGa_{1-x}As$//Si solar cells with 3.5% and 7.5% Al in the middle junction. The inset shows the 4 cm^2 cell under solar simulator. The device parameters are listed in the table. (b) Corresponding EQE with subcells integrated J_{sc} under AM1.5g. The curves are scaled according to the measured J_{sc}.

under spectrally matched 1-sun AM1.5g conditions [21] using a shadow mask of the same aperture as the cell to suppress potential contributions from the silicon wafer outside the cell area. Note that all measurements presented here are based on the full aperture area of the mask opening and, therefore, include shading by the busbar and the metal fingers. The two cell *I–V* curves are shown in Fig. 4(a), with the corresponding device parameters listed in the table below.

One can see that the device with 3.5% Al subcell reaches a performance of 26.2% efficiency, with $V_{\text{oc}} = 2.902$ V, $J_{\text{sc}} = 10.0$ mA/cm^2, and FF $= 89.8$%, whereas the device with 7.5% Al shows only 24.7% efficiency, with $V_{\text{oc}} = 2.929$ V,

$J_{sc} = 10.1\ \mathrm{mA/cm^2}$, and FF = 83.1%. Since both devices have a similar GaInP top- and Si bottom cell, we can assume that the voltage difference originates mainly from the $Al_xGa_{1-x}As$ middle cell. Consequently, the difference in the bandgap-voltage offset, W_{oc} [22], between the 7.5% Al and the 3.5% Al devices, $W_{oc}(Al_{0.075}Ga_{0.925}As) - W_{oc}(Al_{0.035}Ga_{0.965}As)$, is about 23 mV (calculated from the bandgap-corrected V_{oc} difference of 3J cells), thus suggesting a lower material quality in $Al_{0.075}Ga_{0.925}As$. The experimental EQE gives further information about the subcells, as shown in Fig. 4(b): the 3.5% Al device suffers from significant current mismatch: top and middle cells generate, respectively, 11.8 and 12.0 mA/cm^2, whereas only 10 mA/cm^2 are generated in the bottom Si cell (see the dashed curve). This leads to a boost in the measured fill factor (89.8%), as explained in [23]. For the 7.5% Al device, the middle cell shows a low EQE and the overall current is limited by this $Al_{0.075}Ga_{0.925}As$ subcell. In addition, both devices show a relatively poor Si EQE in the long-wavelength range, suggesting a need for better and more stable Si back-side passivation processes. Therefore, both devices do not reach the potential of the technology.

IV. Improvement in Si Bottom Cell

Increasing the current of the Si bottom cell is key for achieving high-performance GaInP/$Al_xGa_{1-x}As$//Si solar cell devices. Indeed, the 1-sun current density of the silicon bottom subcell is often limiting the overall current density to ~10 mA/cm^2 [15], [16]. Significant losses are attributed to a high recombination velocity at the rear surface of the silicon cell. Thus, we have reviewed our III–V//Si process flow in order to identify the deleterious steps for Si passivation.

We have investigated the impact of GaAs substrate removal (chemical etching), performed after bonding the Si to GaInP/$Al_xGa_{1-x}As$ top cells and before the deposition of AlO_x/SiN_x passivation layers on the Si back side. The effect of this chemical GaAs substrate etching step on the effective lifetime in silicon was studied by quasi-steady-state photoconductance (QSSPC) technique, using double-side symmetrically passivated (AlO_x/SiN_x) p-type FZ-Si wafers [see the inset in Fig. 5(a)]. Three different experimental routes were tested.

1) As a reference, one Si wafer was passivated directly after an HF dip, with no exposure to III–V materials.
2) A second Si sample was exposed to the GaAs substrate etching solution of $H_2O_2 + NH_4OH$. This was used to simulate the same chemical solution as during solar cell processing. This sample, called Si Gen1, was passivated directly after the etching step.
3) Finally, the last sample, called Si Gen2, was additionally cleaned by HF after the $H_2O_2 + NH_4OH$ solution.

Those three sample effective lifetimes, measured at an injection level of 1E15 cm^{-3}, are displayed in Fig. 5(a): The reference sample reaches 3.2 ms, the Si Gen1 lifetime drops to 0.55 ms, and the Si Gen2 sample reaches almost 3.5 ms. From these results, it appears to be clear that the chemical solution used to remove the GaAs growth substrate drastically reduces the passivation quality, but an additional HF dip performed after this GaAs substrate etching and before deposition of the passivation layers is enough to recover the same lifetime level than the reference sample. This can be explained by the formation of an oxide layer at the silicon back side during the silicon solar cell preprocessing as well as the GaAs chemical etching step; the oxide layer can be removed without impacting the sample lifetime if a clean HF dip is performed before passivation.

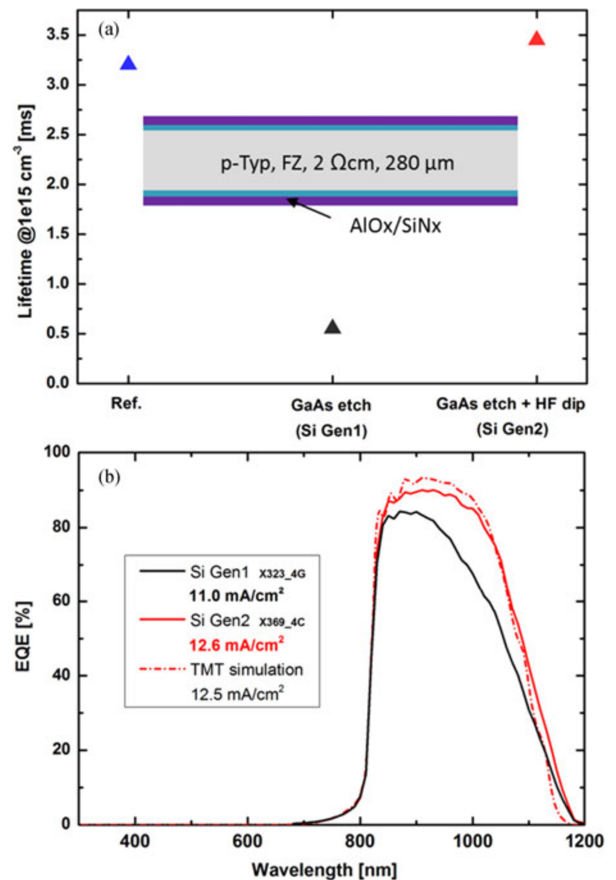

Fig. 5. (a) QSSPC effective lifetime of symmetrically AlO_x/SiN_x passivated FZ-Si wafers. Samples are exposed to three different chemical treatments before passivation: 1) HF dip (Ref. sample); 2) $H_2O_2 + NH_4OH$ (Si Gen1); and 3) $H_2O_2 + NH_4OH$, followed by HF dip (Si Gen2). (b) Bottom cell EQE of GaInP/$Al_{0.075}Ga_{0.925}As$/Si with Si Gen1 (black), Si Gen2 (red), and transfer-matrix optical modeling (dash); corresponding AM1.5g currents are 11.0, 12.6, and 12.5 mA/cm^2.

The Si Gen1 passivation route was the one used for the GaInP/AlGaAs//Si cells presented in Fig. 4. The impact of the Si Gen2 treatment was tested on a new 3J solar cell using the same GaInP/$Al_{0.075}Ga_{0.925}As$ top cells. The comparison of Si bottom cell EQE with the new processing route is shown in Fig. 5(b): the additional HF cleaning step results in a higher EQE over the whole wavelength range between 850 and 1150 nm. Whereas the Si Gen1 bottom cell AM1.5g integrated current density was 11.0 mA/cm^2, the improved passivation results in 12.6 mA/cm^2, which is even above the value of 12.5 mA/cm^2 calculated in the modeling of Section II. Indeed, despite an EQE experimentally slightly lower than expected in the 900–1000-nm region, the near-bandgap EQE is higher than the simulation; this is the evidence of light trapping from the

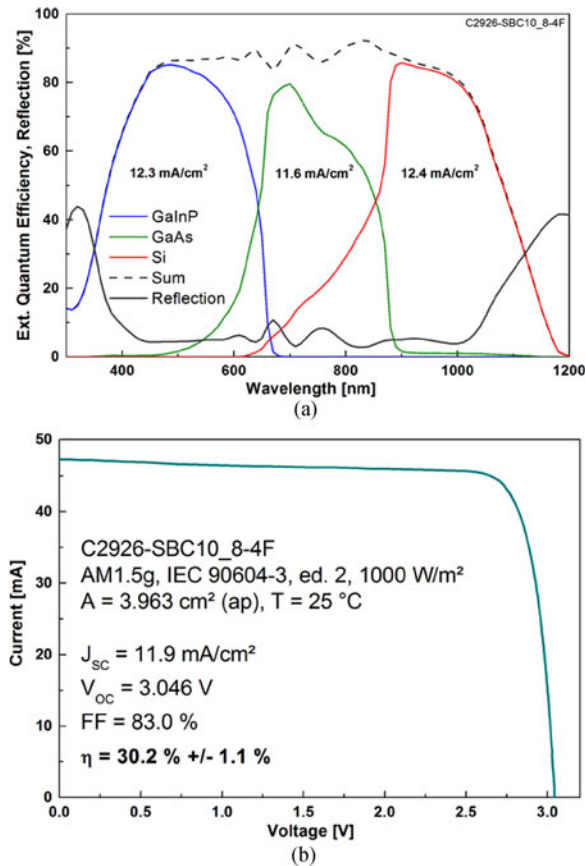

Fig. 6. (a) EQE and reflection of a wafer-bonded GaInP/GaAs//Si device (no Al in the middle junction) implementing a Gen2 silicon bottom cell. Subcell currents are calculated for the AM1.5g spectrum. (b) Corresponding AM1.5g *I–V* characteristics measured under a spectrally adjustable solar simulator at Fraunhofer ISE calibration laboratory with an aperture of 3.963 cm^2. Device parameters are listed in the inset.

unpolished ("etched") silicon back side. The transfer-matrix optical modeling does not simulate this effect; another formalism would be required. OPTOS, for instance, can efficiently simulate noncoherent light propagation and absorption in thick textured sheets [24].

Finally, since it was challenging to grow high-quality AlGaAs cells, we switched to a pure GaAs middle cell. In fact, this is an attractive option since GaAs is less sensitive to impurities (such as oxygen), and high diffusion lengths can be more easily obtained; thus, higher $W_{\rm oc}$ are expected. The voltage decrease between AlGaAs and GaAs cells is, therefore, smaller than their difference in bandgap. In addition, the lower bandgap of GaAs enables to generate the same current density with three times less material compared with $Al_{0.075}Ga_{0.925}As$. We have, therefore, fabricated a III–V//Si 3J solar cell using a 1.7-μm-thin GaInP/GaAs tandem cell structure bonded to a Gen2 Si bottom cell with improved Si passivation. The direct wafer bonding was performed in the EVG580 ComBond cluster. The EQE of the resulting device is shown in Fig. 6(a). The semitransparent GaAs middle cell in combination with the better passivation of Si Gen2 results in a current density of 12.4 mA/cm^2 for the Si bottom cell. The GaAs cell thickness turns out to be slightly too thin and limits the overall device to a current density of 11.6 mA/cm^2. The corresponding *I–V* characteristics, measured at the Fraunhofer ISE calibration laboratory, using an aperture mask of 3.963 cm^2 (busbar and metal finger shading included) are presented in Fig. 6(b). The calibrated efficiency of our best GaInP/GaAs//Si solar cell device is 30.2% $+/-$ 1.1%. This is the first time that a fully integrated monolithic solar cell based on silicon overcomes the single-junction Auger limit for Si solar cells of 29.4% [25].

The open-circuit voltage of this device exceeds 3 V, thanks to a low GaAs $W_{\rm oc}$. However, the FF of only 83.0% is limited by a low shunt resistance in the GaAs cell. This can be seen by an increase of the measured current density close to $J_{\rm sc}$. Here, the GaAs middle cell operates in reverse bias and the low shunt resistance allows the current density to increase from 11.6 mA/cm^2 (determined from the EQE) to a measured value of 11.9 mA/cm^2. Further improvements of the cell characteristics can be expected by increasing the parallel resistance of the GaAs subcell and adjusting the top cell thicknesses to reach better current matching. In addition, it should be possible to get more power out of the silicon bottom cell with advanced passivation and light-trapping features.

V. Summary

We have shown here that surface-activated wafer bonding enables the monolithic integration of III–V layers on silicon. Highly transparent n-GaAs//n-Si bonds with good conductivity are achieved. Moreover, by optimizing the process flow, it was possible to reach fully bonded and nearly defect-free 4-inch Si//GaAs wafer pairs. Monolithic III–V//Si 3J solar cells with different middle cell Al content and thicknesses were simulated and fabricated. GaAs substrate etching was identified as having a negative impact on the rear-side passivation of the Si bottom cell. An additional HF dip enabled recovering a high passivation quality and thus improving the current generation of the silicon bottom cell to 12.6 mA/cm^2 below $Al_{0.075}Ga_{0.925}As$ and 12.4 mA/cm^2 below GaAs. Our best 3J GaInP/GaAs//Si solar cell reaches 30.2% 1-sun AM1.5g efficiency with a 3.963 cm^2 aperture mask. This is a new record value for a monolithic two-terminal III–V//Si tandem solar cell. The path toward higher performances will be continued in the future by implementing a higher bandgap top and middle cells, improving material quality and enhancing absorption and passivation in the silicon bottom cell. With this, 1-sun efficiencies of 35% are realistically achievable.

Acknowledgment

The authors would like to acknowledge K. Wagner, R. Marlene da Silva Freitas, A. Schütte, and R. Koch for depositions and processing, M. Graf for LFC process, and G. Siefer, M. Schachtner, A. Wekkeli, E. Schäffer, and E. Fehrenbacher for solar cell characterization.

References

[1] Kaneka Corp., "World's highest conversion efficiency of 26.33% achieved in a crystalline silicon solar cell," News Release, Sep. 2016.

[2] M. A. Green, K. Emery, Y. Hishikawa, W. Warta, and E. D. Dunlop, "Solar cell efficiency tables (version 48)," *Prog. Photovoltaics, Res. Appl.*, vol. 24, no. 7, pp. 905–913, Jul. 2016.

[3] J. P. Connolly, D. Mencaraglia, C. Renard, and D. Bouchier, "Designing III–V multijunction solar cells on silicon," *Prog. Photovoltaics, Res. Appl.*, vol. 22, no. 7, pp. 810–820, Jul. 2014.

[4] I. Mathews, D. O'Mahony, B. Corbett, and A. P. Morrison, "Theoretical performance of multi-junction solar cells combining III-V and Si materials," *Opt. Exp.*, vol. 20, no. S5, pp. A754–A764, Sep. 2012.

[5] Y. B. Bolkhovityanov and O. P. Pchelyakov, "GaAs epitaxy on Si substrates: Modern status of research and engineering," *Phys.-Uspekhi*, vol. 51, no. 5, May 2008, Art. no. 437.

[6] M. Umeno, T. Kato, T. Egawa, T. Soga, and T. Jimbo, "High efficiency AlGaAs/Si tandem solar cell over 20%," *Sol. Energy Mater. Sol. Cells*, vols. 41/42, pp. 395–403, Jun. 1996.

[7] T. J. Grassman, D. J. Chmielewski, S. D. Carnevale, J. A. Carlin, and S. A. Ringel, "GaAs0.75P0.25/Si dual-junction solar cells grown by MBE and MOCVD," *IEEE J. Photovoltaics*, vol. 6, no. 1, pp. 326–331, Jan. 2016.

[8] F. Dimroth *et al.*, "Comparison of direct growth and wafer bonding for the fabrication of GaInP/GaAs dual-junction solar cells on silicon," *IEEE J. Photovoltaics*, vol. 4, no. 2, pp. 620–625, Mar. 2014.

[9] R. Cariou *et al.*, "Low temperature plasma enhanced CVD epitaxial growth of silicon on GaAs: A new paradigm for III-V/Si integration," *Sci. Rep.*, vol. 6, May 2016, Art. no. 25674.

[10] J. R. Lang, J. Faucher, S. Tomasulo, K. N. Yaung, and M. L. Lee, "Comparison of GaAsP solar cells on GaP and GaP/Si," *Appl. Phys. Lett.*, vol. 103, no. 9, Aug. 2013, Art. no. 092102.

[11] I. Mathews *et al.*, "Adhesive bonding for mechanically stacked solar cells," *Prog. Photovoltaics, Res. Appl.*, vol. 23, no. 9, pp. 1080–1090, Sep. 2015.

[12] S. Essig *et al.*, "Realization of GaInP/Si dual-junction solar cells with 29.8% 1-sun efficiency," *IEEE J. Photovoltaics*, vol. 6, no. 4, pp. 1012–1019, Jul. 2016.

[13] X. Sheng *et al.*, "Printing-based assembly of quadruple-junction four-terminal microscale solar cells and their use in high-efficiency modules," *Nature Mater.*, vol. 13, no. 6, pp. 593–598, Jun. 2014.

[14] K. Xiong *et al.*, "AlGaAs/Si dual-junction tandem solar cells fabricated by epitaxial lift-off and print transfer-assisted bonding," in *Proc. 42nd IEEE Photovoltaic Spec. Conf.*, 2015, pp. 1–3.

[15] S. Essig *et al.*, "Wafer-bonded GaInP/GaAs//Si solar cells with 30% efficiency under concentrated sunlight," *IEEE J. Photovoltaics*, vol. 5, no. 3, pp. 977–981, May 2015.

[16] N. Shigekawa *et al.*, "Current–voltage and spectral-response characteristics of surface-activated-bonding-based InGaP/GaAs/Si hybrid triple-junction cells," *Jpn. J. Appl. Phys.*, vol. 54, Aug. 2015, Art. no. 08KE03.

[17] S. Essig and F. Dimroth, "Fast atom beam activated wafer bonds between n-Si and n-GaAs with low resistance," *ECS J. Solid State Sci. Technol.*, vol. 2, no. 9, pp. Q178–Q181, Jan. 2013.

[18] E. Schneiderlöchner, R. Preu, R. Lüdemann, and S. W. Glunz, "Laser-fired rear contacts for crystalline silicon solar cells," *Prog. Photovoltaics, Res. Appl.*, vol. 10, no. 1, pp. 29–34, Jan. 2002.

[19] D. Häussler *et al.*, "Aberration-corrected transmission electron microscopy analyses of GaAs/Si interfaces in wafer-bonded multi-junction solar cells," *Ultramicroscopy*, vol. 134, pp. 55–61, Nov. 2013.

[20] S. Heckelmann, D. Lackner, C. Karcher, F. Dimroth, and A. W. Bett, "Investigations on $Al_x Ga_{1-x} As$ solar cells grown by MOVPE," *IEEE J. Photovoltaics*, vol. 5, no. 1, pp. 446–453, Jan. 2015.

[21] M. Meusel, R. Adelhelm, F. Dimroth, A. W. Bett, and W. Warta, "Spectral mismatch correction and spectrometric characterization of monolithic III–V multi-junction solar cells," *Prog. Photovoltaics, Res. Appl.*, vol. 10, no. 4, pp. 243–255, Jun. 2002.

[22] R. R. King *et al.*, "Band gap-voltage offset and energy production in next-generation multijunction solar cells," *Prog. Photovoltaics, Res. Appl.*, vol. 19, no. 7, pp. 797–812, Nov. 2011.

[23] G. Siefer *et al.*, "Influence of the simulator spectrum on the calibration of multi-junction solar cells under concentration," in *Proc. 29th IEEE Photovoltaic Spec. Conf.*, 2002, pp. 836–839.

[24] N. Tucher *et al.*, "3D optical simulation formalism OPTOS for textured silicon solar cells," *Opt. Exp.*, vol. 23, no. 24, pp. A1720–A1734, Nov. 2015.

[25] A. Richter, M. Hermle, and S. W. Glunz, "Reassessment of the limiting efficiency for crystalline silicon solar cells," *IEEE J. Photovoltaics*, vol. 3, no. 4, pp. 1184–1191, Oct. 2013.

Romain Cariou studied physics at ENS Cachan and Pierre-and-Marie-Curie University, France. He received the master's degree in applied physics from Ecole Centrale Paris, France, in 2010 and the Ph.D. degree in physics from Ecole Polytechnique, Palaiseau, in 2014, with a thesis on low-temperature epitaxial growth of Si (Ge) materials on Si & GaAs. This joint Ph.D. research was performed with the Laboratory of Physics of Interfaces & Thin Films (LPICM-CNRS) and Alcatel-Lucent Bell Labs France (III-VLab).

In 2015, he joined the Fraunhofer Institute for Solar Energy Systems (ISE), Freiburg, Germany, with a Marie Curie research project focusing on III–V/Si multijunction cells.

Jan Benick studied microsystems technology with the University of Freiburg, Freiburg, Germany. He received the Ph.D. degree from the University of Freiburg/Fraunhofer ISE, Freiburg, in 2010.

He is the Head of the team for innovative cleanroom technologies for high-efficiency silicon solar cells with Fraunhofer ISE.

Paul Beutel received the Diploma degree in mechanical engineering from Lübeck University of Applied Science, Lübeck, Germany, in 2010.

Since 2011, he has been a Process Engineer for metal–organic vapor phase epitaxy with the department "Materials—Solar Cells and Technologies" with the Fraunhofer ISE, Freiburg, Germany. His work focuses on the development and optimization of III–V materials for multijunction solar cells based on InP and GaAs.

Nasser Razek received the Ph.D. degree in solid state physics from Leipzig University, Germany, in 2005.

He joined the technology development team at EV Group headquarters, St. Florian, Austria, in 2013. His current work at EVG focuses on development of permanent wafer bonding technology for many applications (multijunction solar cells, high power devices, SAW filter devices, SOI, and MEMS).

Christoph Flötgen received the Dipl.Phys. degree in applied plasma physics from the Ruhr University Bochum, Bochum, Germany, in 2009. He is currently working toward the Ph.D. degree in covalent wafer bonding with Johannes Kepler University Linz, Linz, Austria.

He is a member of the technology development team with EV Group, St. Florian, Austria. He started as a Process Technology Engineer in 2009, where he was responsible for general permanent wafer-bonding processes with emphasis on plasma-activated direct wafer bonding. His current work covers wafer-bonding process research and development. He has authored and coauthored several papers and presentations in these areas.

Martin Hermle received the Diploma degree in physics from Karlsruhe Institute of Technology, Karlsruhe, Germany, in 2003 and the Ph.D. degree in physics from the University of Konstanz, Konstanz, Germany, in 2008.

He joined the Fraunhofer Institute for Solar Energy Systems, Freiburg, Germany, in 2002. Since 2008, he has been the Head of the "High Efficiency Silicon Solar Cell" Department. His main research interests include the development of solar cell technologies for high-efficiency silicon solar cells and the analysis, characterization, and modeling of silicon and III/V solar cells.

David Lackner received the Ph.D. degree in physics from Simon Fraser University, Burnaby, BC, Canada, in 2011.

In 2011, he joined the Fraunhofer Institute for Solar Energy Systems, Freiburg, Germany, to focus his research on the epitaxy of arsenides, phosphides, and antimonides for solar cell applications and advanced III–V material characterization methods. He is the head of the team "III-V Epitaxy and Material Research" with the Fraunhofer Institute for Solar Energy Systems.

Stefan W. Glunz (M'10–SM'14) received the Ph.D. degree from the University of Freiburg, Freiburg, Germany, in 1995.

He is the Director of the "Solar Cells—Development and Characterization" Division, Fraunhofer Institute for Solar Energy Systems, Freiburg, Germany, and a Professor of photovoltaic energy conversion with the Albert Ludwigs University of Freiburg. His research interests include the design, fabrication, and analysis of high-efficiency solar cells. He is the author/coauthor of more than 100 journal papers in the field of photovoltaics.

Prof. Glunz is the Founding Editor of the IEEE JOURNAL OF PHOTOVOLTAICS. He received the Eni Award for the promotion of science and technology in the field of renewable energies in 2008 and the Becquerel Award for Outstanding Merits in Photovoltaics in 2014.

Andreas W. Bett (M'11) received the Diploma degree in physics and the Diploma degree in mathematics from the Albert Ludwigs University of Freiburg, Freiburg, Germany, in 1988 and 1989, respectively, and the Ph.D. degree in physics from the University of Konstanz, Konstanz, Germany, in 1992.

He joined the Fraunhofer Institute for Solar Energy Systems, Freiburg, in 1987, where he was the Head of the group "III–V Epitaxy and Solar Cells" from 1993 to 2007 and has been the Head of the department "Materials–Solar Cells and Technology" since 2007. His main research interests include the epitaxial growth of III–V semiconductors, characterization techniques, and the development of technologies for the fabrication of devices such as solar cells. His current research is focused on the investigation of concentrator solar cells, modules and systems, multijunction solar cells, and concentrator photovoltaics demonstration projects.

Dr. Bett received the 17th European Becquerel Prize for outstanding merits in photovoltaics in 2009. In 2010, he received the Joseph von Fraunhofer Prize and the EARTO Prize, and in 2012, he received the German Environmental Prize for his efforts and achievements in industrialization of CPV technology.

Markus Wimplinger received his education in electrical engineering from HTL Braunau, Braunau am Inn, Austria.

In 2001, he joined EV Group, Florian am Inn, Austria, as a Project Manager with focus on customer projects, where he is currently the Corporate Technology Development and IP Director. In this role, he oversees EV Group's global Process Engineering team. His further responsibilities include the management of R&D partnerships and contracts with third-party organizations such as companies or government related entities, as well as Intellectual Property affairs associated with EVG's process technology development efforts. In 2003, he transitioned to EV Group North America, Tempe, AZ, USA, where he was the Director Technology North America until August 2006. His past work includes involvement in design, development, and process technology and many other aspects of capital equipment production with both EV Group and at his former job with a capital equipment supplier for nonsemiconductor-related industries. With EV Group, he was involved in 3-D integration-related projects.

Frank Dimroth (M'13) received the Diploma degree in physics from the University of Zurich, Zürich, Switzerland, in 1996 and the Ph.D. degree in physics from the University of Konstanz, Konstanz, Germany, in 2000.

He is the Head of the department "III-V Epitaxy and Solar Cells" with the Fraunhofer Institute for Solar Energy Systems, Freiburg, Germany. His department carries out applied research in the fields of III–V multijunction solar cells and concentrator photovoltaic systems. He developed space and concentrator solar cells with efficiencies up to 46% at 500 suns. He has published more than 200 scientific papers.

Dr. Dimroth and his team received the Fraunhofer Prize in 2010, the French Louis D Science Award in 2010, and the French-German Economy Prize in 2011. He is an Editor for the IEEE JOURNAL OF PHOTOVOLATICS in the field of III–V, concentrator, and space PV.